3-2007

Dynamics of asynchronous random Boolean networks with asynchrony generated by stochastic processes

Xutao Deng
University of Nebraska at Omaha

Huimin Geng
University of Nebraska at Omaha

Mihaela Teodora Matache
University of Nebraska at Omaha, dvelcsov@unomaha.edu

Dynamics of Asynchronous Random Boolean Networks with Asynchrony Generated by Stochastic Processes

Xutao Deng[1], Huimin Geng[1], Mihaela Teodora Matache[2]*

[1] Department of Computer Science, University of Nebraska at Omaha, Omaha, NE 68182-0243, USA

[2] Department of Mathematics, University of Nebraska at Omaha, Omaha, NE 68182-0243, USA

*dmatache@mail.unomaha.edu

Abstract An asynchronous Boolean network with N nodes whose states at each time point are determined by certain parent nodes is considered. We make use of the models developed by Matache and Heidel (M.T. Matache, J. Heidel, "Asynchronous random Boolean network model based on elementary cellular automata rule 126", Phys. Rev. E 71, 026232 (2005)) for a constant number of parents, and Matache (Matache M.T., "Asynchronous Random Boolean Network Model with Variable Number of Parents based on Elementary Cellular Automata Rule 126", IJMPB, Vol. 20, 8 (2006), p. 897-923) for a varying number of parents. In both these papers the authors consider an asynchronous updating of all nodes, with asynchrony generated by various random distributions. We supplement those results by using various stochastic processes as generators for the number of nodes to be updated at each time point. In this paper we use the following stochastic processes: Poisson process, random walk, birth and death process, Brownian motion, and fractional Brownian motion. We study the dynamics of the model through sensitivity of the orbits to initial values, bifurcation diagrams, and fixed-point analysis. The dynamics of the system show that the number of nodes to be updated at each time point is of great importance, especially for the random walk, the birth and death, and the Brownian motion processes. Small or moderate values for the number of updated nodes generate order, while large values may generate chaos depending on the underlying parameters. The Poisson process generates order. With fractional Brownian motion, as the values of the Hurst parameter increase, the system exhibits order for a wider range of combinations of the underlying parameters.

1. Introduction

A large class of biological networks, cellular automata, or artificial neural networks have been modelled as Boolean networks in recent years (Aldana et al., 2003), (Andrecut and Ali, 2001),

(Anthony, to appear), (De Garis et al., 2002), (Fox and Hill, 2001), (Heidel et al., 2003), (Huang, 2001), (Huepe and Aldana, 2002), (Kürten, 1988), (Matache and Heidel, 2004), (Matache and Heidel, 2005), (Matache, 2006), (Silvescu and Honavar, 2001), (Shmulevich et al., 2002). The Boolean models are easy to understand and relatively easy to handle. General interest in Boolean networks and their applications in biology and automata networks started much earlier (Boccara et al., 1994), (Flyvbjerg and Kjaer, 1988), (Fogelman-Soulie et al., 1982), (Fogelman-Soulie, 1984), (Kauffman, 1993), (Sherlock, 1979), (Stauffer, 1988), with publications such as the one by Kauffman (1993), whose work on the self-organization and adaptation in complex systems has inspired many other research studies. It is important to understand and study the dynamics of Boolean networks in order to use them for simulation and prediction of the real networks they model.

The present work is an extension of previous work by Matache and Heidel (2004) and Matache (2006). Those papers generalize rule 126 of elementary cellular automata (ECA) (Wolfram, 2002) and provide models for the probability of finding a node in state 1 (or ON) at time t. Rule 126 can be very simply described in terms of cell evolution as follows: complete crowding of live, ON, cells causes death, OFF, in the next generation, while complete isolation of a cell prevents birth in the next generation (Matache and Heidel, 2004) . In other words if a node and each of its parents are all ON or all OFF then the node turns OFF at the next time step; otherwise it turns ON.

Various authors have observed that for many biological phenomena or cellular automata, asynchronous versions are more plausible models than synchronous ones. For example, individual ants display aperiodic patterns of active and resting periods, while the colony as a whole may exhibit synchronized activity; asynchronous activity of the neurons in the brain could lead to some global patterns (Cornforth et al., 2002). At the same time, "Type A" spiking neurons with "binary encoding" in which the neurons have "active" and "non-active" periods (Anthony, to appear) generate asynchronous dynamics in a neural network. In (Stark and Hughes, 2000) the authors show that asynchrony in cellular automata is a realistic approach to modelling biological information processing. They note that "in the absence of human intervention and invention, nature is asynchronous". At the same time it has been observed that asynchronous random Boolean networks can be a good choice for modelling both rhythmic and non-rhythmic phenomena, while using an updating scheme that generates uniform average time delays and independent updating for all nodes (Di Paolo, 2001). The topology of rhythm in such networks is

further studied in (Rohlfshagen and Di Paolo, 2004). Asynchrony in cellular automata has also been studied in (Schönfisch and De Roos, 1999). In the paper (Matache and Heidel, 2005) the authors consider an asynchronous Boolean network with N nodes, each node having a number of parents that is fixed for all nodes. In (Matache, 2006) the author allows for a varying number of parents, generalizing results in (Matache and Heidel, 2005); in both these papers the asynchrony is generated using some classical random variables, including the uniform, binomial, Poisson, power law, and hypergeometric distributions. These distributions represent a more general updating scheme than the ones used so far in the literature, e.g. the clock scheme (DiPaolo, 2001), (Low and Lapsley, 1999), (Thomas, 1979), the cyclic scheme (Kanada, 1994), the random independent scheme (Harvey and Bossomaier, 1997), and the random order scheme (Harvey and Bossomaier, 1997). It has been shown in (Cornforth et al., 2002) that properties of the models are changed by the particular update scheme chosen. In this paper we go one step further with the generalization and assume that the updating of the nodes is done according to certain stochastic processes so that the distributions generating the number of nodes to be updated can change with time. Thus we provide further insights into the dynamics of the Generalized Asynchronous Random Boolean Networks (GARBN) (Gershenson, 2002), which can update any number of nodes, chosen at random, at each time step.

We make use of the Boolean rule mentioned above, namely if a node of the network and each of its parents have the same value (0 or 1) at time t, then the value of the node at the next time step $t+1$ is 0; otherwise it is 1. We discuss the formulae for the probability of finding a node in state 1 at time t in Section 2. The most general formula for the probability $p(t+1)$ that a node is in state 1 at time $t+1$ given $p(t)$ is

$$p(t+1) = \sum_{j=1}^{J} \frac{M_j}{N} \left[\frac{p_j(t)}{\frac{M_j}{N}} \left(1 - \frac{x_t}{N} \left(1 - (1-p(t))^{k_j} + p(t)^{k_j} \right) \right) + \frac{x_t}{N} \left(1 - (1-p(t))^{k_j} \right) \right]$$

where N is the size of the network, x_t is the number of nodes updated at time t, $k_1, k_2, \ldots, k_J$ are the distinct values for the number of parents of the nodes, M_j is the number of nodes with k_j parents, and $p_j(t)$ is the probability of finding a node having k_j parents in state 1 at time t. In Section 3 we provide an overview of the stochastic processes used for generating asynchrony, and we use simulation methods to generate consecutive states of the network for both the real system and the model using these processes. The results from the model match the results from the system very well. In Section 4 we study the dynamics of the model through the analysis of the sensitivity of the orbits to the initial values and bifurcation diagrams. In the

first three subsections of Section 4 we use Poisson, random walk, and certain birth and death processes as the random number generators for the number x_t of nodes to be updated at each time point t. We show that the system exhibits ordered behavior mostly for small and medium values of x_t, while for large values it might exhibit chaos for certain parameter combinations. In the synchronous case we show that the system's behavior matches the previous findings of (Matache and Heidel, 2004). In 4.4 we extend our analysis to asynchrony generated by the Brownian motion and fractional Brownian motion processes to understand the dynamics of the system when the number of nodes to be updated has special properties, such as long-range dependence and self-similarity. We show that the values of x_t together with the Hurst parameter are important in the dynamics of the system. Section 5 is dedicated to conclusions and possibilities for future work.

2. The Random Boolean Network Model

In this section we describe the Boolean model. Significant results from (Matache and Heidel, 2005) and (Matache, 2006) are recalled.

Consider a network with N nodes. Each node c_n, $n = 1, 2, \ldots, N$, can have only two values, 1 or 0. Often this is interpreted as a system in which each node can be either ON or OFF. At each time point t the system can be in one of the 2^N possible states. We assume the network is asynchronous; that is, not all nodes are necessarily updated at each time point. The evolution of the nodes from time t to time $t+1$ is given by a Boolean rule which is considered the same for all nodes. Each node c_n is assigned a random "neighborhood" of parents, whose values at time t influence the value of c_n at time $t+1$ through the following Boolean rule. If c_n and each of its parents have the same value at time t (that is they are all either 0 or 1), then $c_n(t+1) = 0$, otherwise $c_n(t+1) = 1$. This generalizes rule 126 of cellular automata (Matache and Heidel, 2004, 2005), (Wolfram, 2002). The parents of a node are chosen randomly from the remaining $N-1$ nodes and do not change thereafter. More precisely, if a node has k parents, then a set of k nodes is chosen from the remaining $N-1$ nodes with probability $\frac{1}{\binom{N-1}{k}}$. We are interested in the probability $p(t+1)$ that a node is in state 1 at time $t+1$, given $p(t)$.

In (Matache and Heidel, 2005) the authors show that $p(t+1)$ is given by

$$p(t+1) = p(t) + \frac{1}{N}\left[1 - p(t) - p(t)^{k+1} - (1-p(t))^{k+1}\right] \tag{1}$$

for the asynchronous random Boolean networks (ARBN) case when only one node is updated at each time point, and

$$p(t+1) = p(t) + \frac{x_t}{N}\left(1 - p(t) - (1-p(t))^{k+1} - p(t)^{k+1}\right) \tag{2}$$

for the GARBNs case when a random number of nodes is updated at each time point. In these formulae k is the number of parents of each node (considered fixed), and x_t is the number of nodes to be updated at time t (randomly generated).

In (Matache, 2006) the formula above is generalized for an arbitrary number of parents for each node. It is shown that the probability that a node is in state 1 at time $t+1$ is given by

$$p(t+1) = \sum_{j=1}^{J} \frac{M_j}{N}\left[\frac{p_j(t)}{\frac{M_j}{N}}\left(1 - \frac{x_t}{N}\left(1-(1-p(t))^{k_j} + p(t)^{k_j}\right)\right) + \frac{x_t}{N}\left(1-(1-p(t))^{k_j}\right)\right] \tag{3}$$

where M_j is the number of nodes that have k_j parents, with $j = 1, 2, \ldots, J$, and $k_1, k_2, \ldots, k_J$ are the distinct number of parents the N nodes have. Also, x_t is again the number of nodes to be updated at time t, and is randomly generated. We can observe the similarities with the model in (Matache and Heidel, 2005) if we collect together the terms involving $\frac{x_t}{N}$.

The following simulation algorithm is proposed for the Boolean network under consideration. The algorithm provides the computation of $p(t)$ for all $t = 0, 1, 2, \ldots$.

- For $t = 0$ choose arbitrary numbers $p_j(0) \in [0, \frac{M_j}{N}]$, $j = 1, 2, \ldots, J$, and let
$$p(0) = \sum_{j=1}^{J} p_j(0).$$
- For each $t = 0, 1, 2, \ldots$ compute
$$p_j(t+1) = \frac{M_j}{N}\left[\frac{p_j(t)}{\frac{M_j}{N}}\left(1 - \frac{x_t}{N}\left(1-(1-p(t))^{k_j} + p(t)^{k_j}\right)\right) + \frac{x_t}{N}\left(1-(1-p(t))^{k_j}\right)\right] \tag{4}$$
where $j = 1, 2, \ldots, J$, and
$$p(t+1) = \sum_{j=1}^{J} p_j(t+1).$$

The formula for $p_j(t)$ in (4) is similar to the summands of $p_j(t)$ in (3).

We use this simulation algorithm to see how well the model matches the real system in the case when x_t is generated by a stochastic process. We will be using integer-valued processes including certain Poisson, random walk, and birth and death processes (as special Markov processes), to illustrate how the iterations of the model match the iterations of the system. In studying the dynamics of the system through the model analysis, we will expand our interest also to the

Brownian motion and the fractional Brownian motion processes, which are not integer-valued. Thus we provide a deeper understanding of how the maps of the models behave considering a wider variety of processes with various properties.

The fixed points of the multidimensional map (3) are obtained by solving the system

$$p_j = \frac{M_j}{N}\left[\frac{p_j}{\frac{M_j}{N}}\left(1-\frac{x_t}{N}\left(1-\left(1-\sum_{i=1}^{J}p_i\right)^{k_j}+\left(\sum_{i=1}^{J}p_i\right)^{k_j}\right)\right)+\frac{x_t}{N}\left(1-\left(1-\sum_{i=1}^{J}p_i\right)^{k_j}\right)\right]$$

where $j=1,2,\ldots,J$. By direct computations, the equivalent system

$$p_j = \frac{\frac{M_j}{N}\left(1-\left(1-\sum_{i=1}^{J}p_i\right)^{k_j}\right)}{1-\left(1-\sum_{i=1}^{J}p_i\right)^{k_j}+\left(\sum_{i=1}^{J}p_i\right)^{k_j}}, \qquad j=1,2,\ldots,J \tag{5}$$

indicates that if $k_j \to \infty$ for a fixed j, then p_j converges to $\frac{M_j}{N}$. Also, $p_j = 0, j = 1,2,\ldots,J$ is obviously a fixed point of the J-dimensional map. If for a given $j=1,2,\ldots,J$ we set $k_j = 1$ then $p_j = \frac{1}{2}\frac{M_j}{N}$. On the other hand, if none of the k's are equal to 1, then since $p_j \to \frac{M_j}{N}$ as $k_j \to \infty$ the sum $\sum_{j=1}^{J} p_j \to 1$ as the values k_j increase. The fixed points are independent of the choice of x_t.

3. Review of some Stochastic Processes and Simulations

Given the variety of stochastic processes that one could consider, we narrow our study to several examples of processes that generalize the distributions used in (Matache and Heidel, 2005) and (Matache, 2006) or represent natural choices for applications to biology, genetics, physics, chemistry or sociology. We focus first on integer-valued processes, and later apply also some non integer-valued processes for studying the dynamics of the system.

Definition 1 A counting process $\{N(t), t \geq 0\}$ is called a Poisson process with rate $\lambda > 0$ if the process starts at 0, i.e. $N(0) = 0$, and has independent increments, and the number of events in a time interval of length t is Poisson distributed with mean λt.

If the arrival rate λ is a constant the process is said to be homogeneous, while if λ is a function of time t it is said to be nonhomogeneous. We will explore examples from each of these types of Poisson processes. For more on the Poisson process one can check any introductory book on stochastic processes (e.g. (Ross, 1983) or (Taylor and Karlin, 1998)).

For the nonhomogeneous Poisson process we look at a power function for the intensity parameter

$$\lambda(t) = \alpha t^{-\beta}$$

where α and β are positive constants. The larger the β, the steeper the decrease in the values of x_t, which approach a rather stable range in which these values fluctuate as t increases. This would correspond to a situation in which there is an initial burst of activity of the nodes, followed by a diminishing trend that reaches a more or less stable behavior.

Definition 2 If $X_1, X_2, X_3, \ldots$ are independent and identically distributed random variables with $\mathbf{P}(X_i = j) = a_j, j = \ldots, -1, 0, 1, \ldots$, and if we define $S_0 = 0$ and $S_n = \sum_{i=1}^{n} X_i$, then the process $\{S_n, n \geq 1\}$ is a Markov chain with $P_{ij} = a_{j-i}$ and is called the general random walk process.

We will employ the one-step symmetric random walks, that is, if we regard the state of the system as the position of a moving particle, then the particle can move from state i only to states $i-1$ and $i+1$ with equal probability. More information on random walks can be found in (Ross, 1983) or (Taylor and Karlin, 1998).

Definition 3 A birth and death process $\{X(t), t \geq 0\}$ is a Markov process on the states $0, 1, 2, \ldots$, with stationary transition probabilities $P_{ij}(t) = \mathbf{P}(X(t+s) = j | X(s) = i)$ for all $s \geq 0$, having the following properties:

(i) $P_{i,i+1}(h) = \lambda_i h + o(h)$ as $h \to 0$, $i \geq 0$;

(ii) $P_{i,i-1}(h) = \mu_i h + o(h)$ as $h \to 0$, $i \geq 1$;

(iii) $P_{i,i}(h) = 1 - (\lambda_i + \mu_i)h + o(h)$ as $h \to 0$, $i \geq 0$;

(iv) $P_{ij}(0) = \delta_{ij}$;

(v) $\mu_0 = 0, \lambda_0 > 0, \mu_i, \lambda_i > 0, i = 1, 2, \ldots$.

The process $X(t)$ represents the size at time t of a population with birth rates λ_i and death rates μ_i. We will focus on one example of such processes described in (Taylor and Karlin, 1998).

Example 1 The logistic process assumes that the size of the population $X(t)$ ranges between two fixed bounds $L_1 < L_2$ for all time points t. The members of the population act independently of each other and the birth and death rates for the population are $\lambda_n = \alpha n(L_2 - n)$ and $\mu_n = \beta n(n - L_1)$. The stationary distribution is given by

$$\pi_{L_1+m} = \frac{c}{L_1 + m} \binom{L_2 - L_1}{m} \left(\frac{\alpha}{\beta}\right)^m, \qquad m = 0, 1, 2, \ldots, L_2 - L_1$$

where c is a constant such that π is a probability distribution.

Definition 4 A process $\{B^H(t), t \in \mathbf{R}\}$ is called a standard fractional Brownian motion (FBM) with Hurst parameter $H \in (0, 1)$ if it is a Gaussian process such that

$$\mathbf{E}[B^H(t)] = 0$$

and

$$\mathbf{Cov}[B^H(t), B^H(s)] = \frac{1}{2}\left[|t|^{2H} + |s|^{2H} - |t-s|^{2H}\right]$$

where $s, t \in \mathbf{R}$.

If $H = \frac{1}{2}$ the resulting process is the classical Brownian motion (BM). The FBM process has some important properties as stated below.

Properties Let $\{B^H(t), t \in \mathbf{R}\}$ be a standard FBM. Then:

(i) $B^H(t)$ is standard normal with mean 0 and variance $|t|^{2H}$.

(ii) The process has stationary increments, i.e. $\forall s, t > 0$ the increments $B^H(t+s) - B^H(t)$ and $B^H(s)$ have the same distribution.

(iii) FBM is a self-similar process with parameter H, i.e. the processes $\{B^H(at), t \geq 0\}$ and $\{a^H B^H(t), t \geq 0\}$ have the same probability law for each a greater than 0. This property is also known as the fractal behavior of the process, since it provides probability law invariance to time scale changes.

(iv) The autocorrelation function $\mathcal{R}(k) = \mathbf{E}[Y(1)Y(k)]$ of the fractional Gaussian noise process, which is the increment of FBM, $\{Y(k) := B^H(k) - B^H(k-1), k = 1, 2, 3, \dots\}$, behaves as a power function for large k. More precisely, $\mathcal{R}(k) \sim H(2H-1)k^{2H-2}$, as $k \to \infty$. If $H \in (\frac{1}{2}, 1)$, $\mathcal{R}(k)$ tends to zero slowly, so that $\sum_k \mathcal{R}(k)$ diverges. Thus the system exhibits the property of long-range dependence.

The last two properties make FBM a natural choice for modeling systems that exhibit both fractal behavior and long-range dependence. Although the FBM is not integer-valued, it helps analyze what happens to our system under the assumption that the number of nodes to be updated at each time point depends on the long-term history of the process x_t. At the same time we make use of the assumption that if we change the time scale, the number of updated nodes follows the same type of distribution. We are interested in seeing if the parameter H makes a difference, and also if there is a significant difference with the BM process which does not exhibit long-range dependence. For more on the BM process see (Ross, 1983) or (Taylor and Karlin, 1998). The FBM process has been studied extensively in the last 15 years, with applications to telecommunications, finance, and queuing systems in general (Beran, 1994), (Duncan et al., 2000), (Leland et al., 1994), (Matache and Matache, 2005), (Willinger et al., 1998), (Yin, 1996). To simulate the FBM process we use the method developed in (Yin, 1996).

Let us start the simulations of the real system and the model to see if there is a good match between them. For the case of a nonconstant number of parents, we provide visual output only for two possible number of parents for each node. The simulations that follow have been obtained using Matlab programs. Although we present only a few graphs, the conclusions have been drawn from numerous simulations. In general we present only typical graphs. We discuss the case of a fixed number of parents separately for a more clear description of the behavior of the system.

The graphs in Figure 1 are typical for the 2-dimensional case. We iterate the system and the model a number of times (specified in the graphs), and plot $p(t+\text{iteration})$ versus $p_1(t)$ and $p_2(t)$. The points represent the real system, while the mesh represents the iterations of the model. In this figure x_t is generated by a symmetric random walk starting at $3N/4$ where $N = 128$. Thus the values of x_t are sufficiently large. The parameters are as follows: $k_1 = 4, k_2 = 64, M_1 = 120$, and $M_2 = 8$. The random walk, the birth and death, and the Poisson process with various parameter combinations generate similar graphs, with slight variations in terms of the shape of the mesh and the rate at which the model becomes a very good match for the real system. For some parameter combinations it takes a number of iterations before the model matches well with the real system. However, in the long run the model is a very good approximation of the Boolean network under consideration. We note here that for the nonhomogeneous Poisson process with a power function for the intensity parameter, namely $\lambda(t) = \alpha t^{-\beta}$, the model is a good approximation of the real system for $\alpha \in [0, N]$ and $\beta > 1$. For lower values of β the system may become synchronous and we observe that the model is not a very good match in this case. However, if the values of α and β are such that the x_t values are small or moderate, the model is a very good match for the system (in the long run), especially for small and moderate connectivity parameters.

In the case of the logistic birth and death process, the model is a good approximation for most situations, except for very large values of x_t.

In Figure 2 we present the one-dimensional case (k is fixed for all nodes). We graph $p(t+\text{iteration})$ versus $p(t)$ where the number of iterations is specified in the graphs. The parameters are $N = 256, k = 4$ and the values of x_t are obtained from a symmetric random walk starting at $3N/4$. We observe the good match of the system and the model. We note that again this graph is typical for x_t generated by a random walk, a birth and death, or a Poisson process with various parameters. Variations of the graphs occur in terms of the rate at which the model

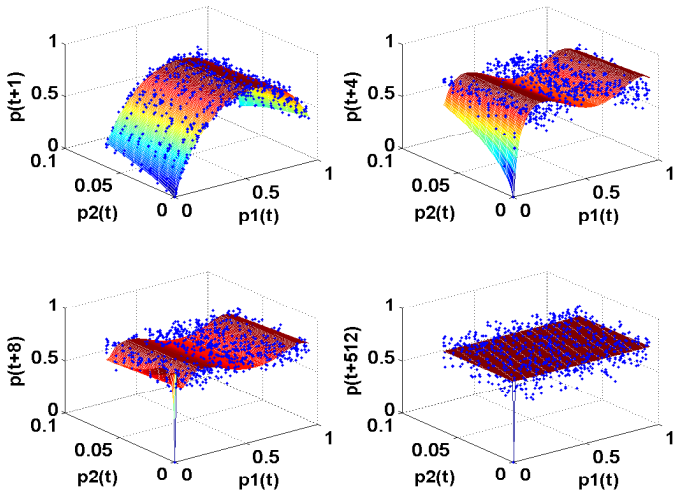

FIGURE 1. Iterations of the system and the model for ARBN, with $N = 128, M_1 = 120, M_2 = 8, k_1 = 4, k_2 = 64$, and x_t from a symmetric random walk process starting at $3N/4$. The values of x_t are sufficiently large. We plot some of the first 512 iterations of the system and the model as specified in the labels. We observe the good match of the system and the model. After 256 iterations, the model and the system reach a somewhat steady behavior.

reaches the steady-state behavior. For example, the rate increases as the parameter λ of the Poisson process increases. Also, the steady-state behavior of the model gets closer to 1 as the parameter k increases. The shape of the transient graphs prior to the steady-state behavior may vary from one case to another but overall we observe a very good match of the model and the system, in numerous cases even a perfect match. Comments regarding the parameters of the nonhomogeneous Poisson process and the logistic process yielding a good match of the model and the system are valid also in this case.

Next we study the dynamics of the system when the asynchrony is generated by the various stochastic processes mentioned above. We discuss each of the processes separately for a better understanding.

4. System Dynamics

4.1. **Asynchrony Generated by a Random Walk Process.** We start our study with the analysis of the sensitivity of the orbits to the initial values. First we consider the case of two distinct values for the number of parents. We fix the parameters $\frac{M_1}{N}, \frac{M_2}{N}, k_1, k_2$, and choose two initial pairs $(p_1(0), p_2(0))$ and $(q_1(0), q_2(0))$ as starting points for the orbits. We iterate many

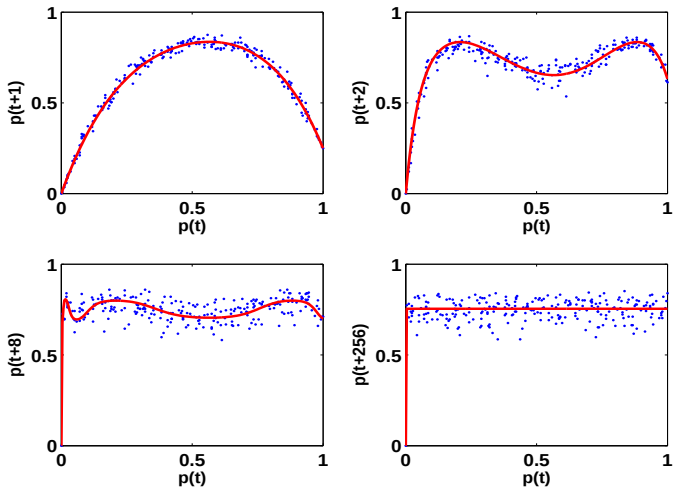

FIGURE 2. Iterations of the system and the model for ARBN, with $N = 256, k = 4$ and x_t from a symmetric random walk process with starting point at $3N/4$. We plot some of the first 256 iterations of the system and the model as specified in the labels. We observe the good match of the system and the model. After 256 iterations, the model and the system reach a more or less steady behavior.

times the equations of the model and compute $p(t) = p_1(t) + p_2(t)$ and $q(t) = q_1(t) + q_2(t)$ for each time point t. Then we plot the error $E(t) = |p(t) - q(t)|$ versus t.

In most cases, the error converges to zero. When the values of x_t are large, and especially when they reach the upper bound N, meaning that the system is actually synchronous, the error might not converge to zero.

In Figure 3, $N = 256, M_1 = \frac{N}{16}, M_2 = \frac{15N}{16}, k_1 = 4$, and $k_2 = 8$. Here x_t is generated by a symmetric random walk starting at $15N/16$. The two initial values are very close. The upper graph shows the sample path of x_t. We see that for most time points t the value of x_t is N, which means that the system is synchronous. For large values of t however, the system is asynchronous. The lower graph is the error plot. We see that the error converges to zero eventually, but it is nonzero while the system is synchronous.

In general, if the values of x_t are small, the error converges very quickly to zero. If the values of x_t are large, then a large connectivity k may wipe out any variation in the error, which converges to zero. However, if the connectivity is small for large values x_t, the error may or may not converge to zero. Even for very similar initial values, the error may fluctuate without settling to zero. If the system is synchronous the error is not converging to zero in most cases.

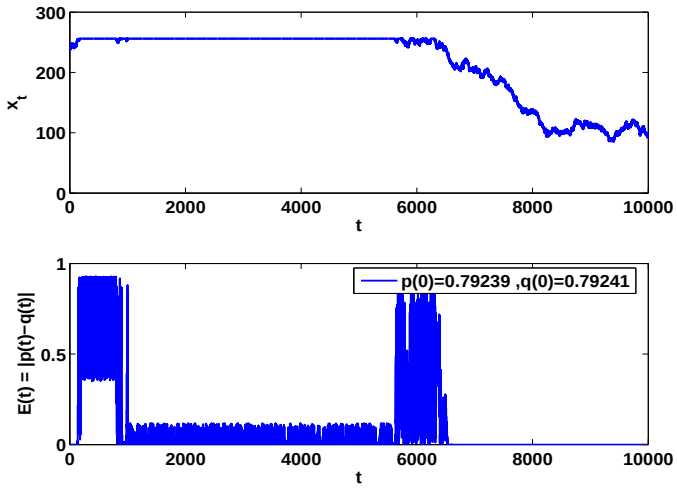

FIGURE 3. Sensitivity of the orbits to the initial values with $N = 256, M_1 = \frac{N}{16}, M_2 = \frac{15N}{16}, k_1 = 4$, and $k_2 = 8$. Here x_t is generated by a symmetric random walk starting at $15N/16$. The upper graph is the sample path of x_t. For most time points t the value of x_t is N, which means that the system is synchronous. For large values of t however, the system is asynchronous. Two initial pairs $(p_1(0), p_2(0))$ and $(q_1(0), q_2(0))$ are chosen as starting points for the orbits. The equations of the model are iterated and the values $p(t) = p_1(t) + p_2(t)$ and $q(t) = q_1(t) + q_2(t)$ are computed for each time point t. Then the error $E(t) = |p(t) - q(t)|$ is plotted versus t in the lower graph. We see that the error converges to zero eventually, but it is nonzero while the system is synchronous.

For the one-dimensional case, when the number of parents is fixed for all nodes, the error converges to zero for small values of x_t. For medium or large values of x_t it converges to zero if k is small enough, and it may or may not converge to zero for larger values of k. In general, we make the observation that for larger values of x_t, the error may converge to zero for small k values, then be nonconvergent for larger values of k, and then again converge to zero for even larger values of k. This suggests that we may expect period-doubling bifurcations and chaos which may be reversed or might exhibit periodic windows in the bifurcation diagrams to follow. We will see that this is indeed the case. Finally, when the system is synchronous, the error converges to zero mainly for large values of k, suggesting that the system may exhibit chaos for small values of k.

The study of the sensitivity of the orbits to the initial values is complemented with a bifurcation diagram analysis. First we consider the two-dimensional case and fix the parameters

M_1, M_2 and N. In Figure 4 we graph bifurcation diagrams of $p(t)$ versus k_2 for several values of k_1 for $N = 512, M_1 = \frac{N}{16}, M_2 = \frac{15N}{16}$.

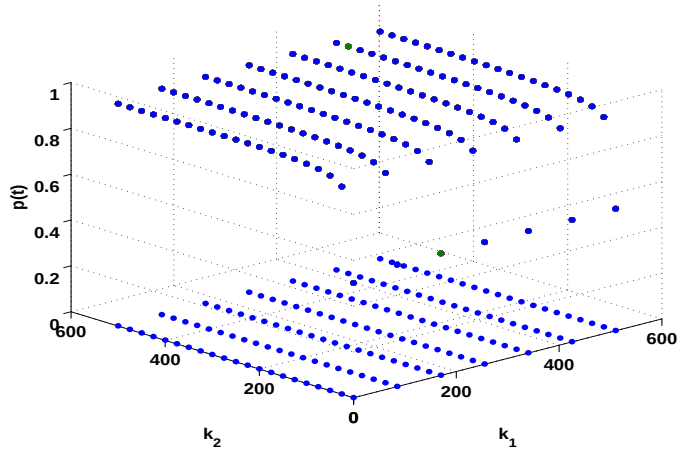

FIGURE 4. Bifurcation diagrams for $N = 512, M_1 = \frac{N}{16}, M_2 = \frac{15N}{16}$, and x_t from a symmetric random walk starting at $N/4$. The equations of the model are iterated 2000 times to eliminate any transient behavior. We plot the bifurcation diagram of $p(t)$ versus k_2 for several values of k_1. We can see that the system exhibits stable fixed points.

The values x_t are from a symmetric random walk starting at $N/4$, so they are rather small. The system exhibits an ordered behavior with stable fixed points. This situation is typical for most combinations. However, if the values of x_t are very large, the system may exhibit order or chaos, and this agrees with the observations for the error plot. For example in Figure 5, $N = 512, M_1 = \frac{N}{16}, M_2 = \frac{15N}{16}$ as before, and x_t is generated by a symmetric random walk starting at $15N/16$, which means that the x_t values are large.

The diagrams show that the system exhibits chaos, with reversed bifurcations and periodic windows. For values of k_1 larger than 250 (not shown in Figure 5), the diagrams are similar to the one for $k_1 = 250$. Thus, large values of k_2 wipe out any instability in the system as long as k_1 is large enough. If one of the parameters is small, the system exhibits chaos in general. However, for very small connectivity values, the system exhibits stable fixed points as seen in the first left slice of the figure.

If the system is synchronous, meaning that $x_t = N$ for all time points t, then the bifurcation diagrams agree with the findings of (Matache and Heidel, 2004) which indicate that chaos occurs for rather small connectivity parameters through cascades of period-doubling bifurcations, which are reversed through period-halving bifurcations as one of the connectivity parameters increases

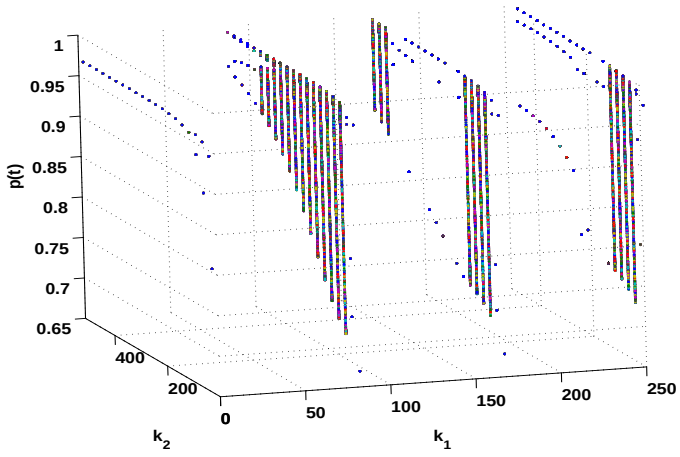

FIGURE 5. Bifurcation diagram for $N = 512, M_1 = \frac{N}{16}, M_2 = \frac{15N}{16}$, and x_t from a symmetric random walk starting at $15N/16$. The equations of the model are iterated 2000 times to eliminate any transient behavior. We plot the bifurcation diagram of $p(t)$ versus k_2 for several values of k_1. The diagrams show that the system exhibits chaos, with reversed bifurcations and periodic windows. For values of k_1 larger than 250 (not shown in the figure), the diagrams are similar to the one for $k_1 = 250$. Thus, large values of k_2 wipe out any instability in the system as long as k_1 is large enough. If one of the parameters is small, the system exhibits chaos in general. However, for very small connectivity values, the system exhibits stable fixed points as seen in the first left slice of the graph.

freely. High connectivity leads to order. We include one bifurcation diagram as a sample in Figure 6.

The bifurcation diagrams have been plotted after iterating the system 2000 times to eliminate transient behavior. However, as noted in the error plots, there may be situations in which order is attained only after many iterations.

In the one-dimensional case, when the value of k is fixed for all nodes, we observe that large values of x_t generate chaos through period-doubling bifurcations, with periodic windows for larger values of the connectivity parameter. We observe that for lower values of x_t the bifurcation diagrams tend to become "thinner" while for small values of x_t the system exhibits order through stable fixed points of period one or period two. We can see this in Figure 7, where the left column shows three different sample paths, with values of x_t that decrease in general from one graph to the next, and the corresponding bifurcation diagrams on the right column. The system is iterated $5N$ times, with $N = 512$.

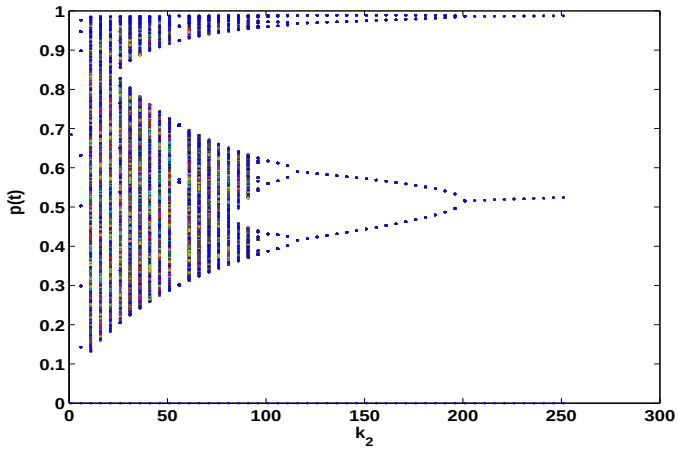

FIGURE 6. Bifurcation diagram for $N = 512, M_1 = \frac{N}{2}$, and $x_t = N$ for all time points t, that is a synchronous system. We observe the chaotic behavior for small values of the second connectivity parameter k_2 for $k_1 = 5$. The route through chaos is through period-doubling bifurcations which are reversed through period-halving bifurcations as observed in (Matache and Heidel, 2004).

For the case of a synchronous network, the system exhibits chaos for small values of k which is reversed, and hence the system exhibits order for large values of the connectivity parameter. This is shown in Figure 8. Since in the case of synchrony $x_t = N$ for all time points t, this result is valid in general, and it matches and supplements the observations in (Andrecut and Ali, 2001) for a one-dimensional synchronous system. We will focus only on the asynchronous systems in the remainder of this paper.

For other parameter combinations, the graphs are similar to the graphs presented here. Thus the bifurcation diagrams emphasize the situation observed in the error plots.

In conclusion, large values of x_t can generate chaos depending on the connectivity parameters, while small values of x_t generate order regardless of the connectivity parameters. These results support the conclusion in (Matache, 2006). Namely, for a fixed probability distribution, by replacing the term $\frac{x_t}{N}$ in the formula (3) by a constant $\alpha \in [0, 1]$, we can view α as the mean value of the distribution generating x_t divided by N. By studying the behavior of the new map obtained this way, the following conclusion is reached: if a small or moderate number of nodes update at the same time, the system is ordered in the long run, while for a large number of nodes updated at the same time, the system can exhibit order or chaos, depending on the other parameters.

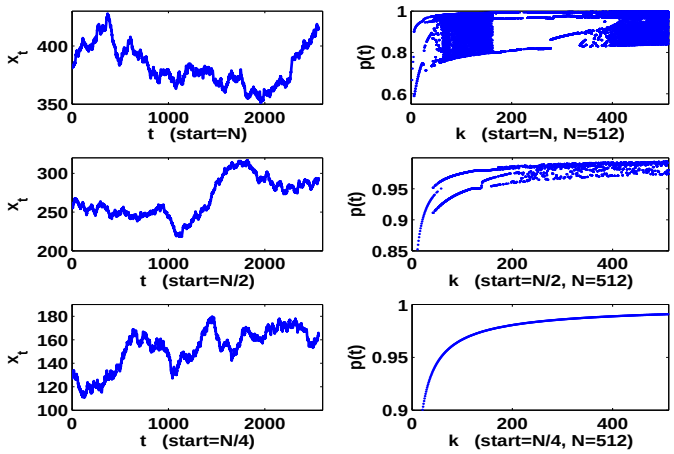

FIGURE 7. Bifurcation diagrams for the one-dimensional case, with a fixed number of parents, with $N = 512$ and x_t from a symmetric random walk starting at $N, N/2$ and $N/4$ respectively. The sample paths are on the left column of graphs. The right column represents the corresponding bifurcation diagrams. The equations of the model are iterated $5N$ times to eliminate any transient behavior. The diagrams show that the system exhibits chaos through period-doubling bifurcations for larger values of x_t, and order for small values of x_t.

In the synchronous case the results match the findings of (Andrecut and Ali, 2001) for the one-dimensional case, and (Matache and Heidel, 2004) for the multidimensional case.

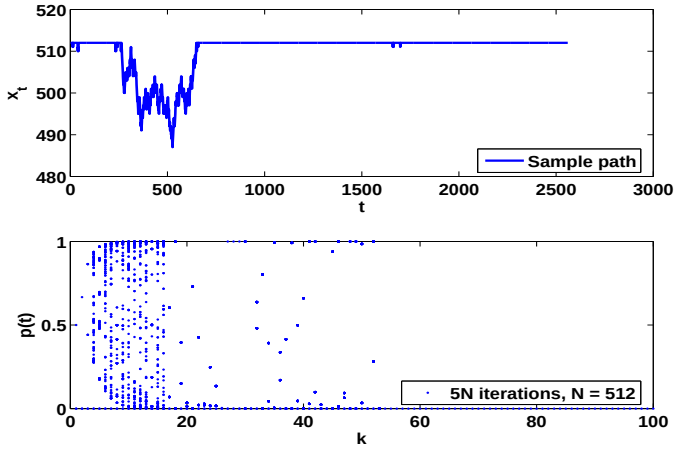

FIGURE 8. Bifurcation diagrams for the one-dimensional case, with a fixed number of parents, with $N = 512$ and x_t from a symmetric random walk starting at N, which makes the system synchronous for most time points. The diagrams show that the system exhibits chaos for small values of k, and order for large values of k.

4.2. **Asynchrony Generated by Certain Birth and Death Processes.** As specified in Section 3, we consider one example of a birth and death process, namely the logistic process.

Let us recall that the logistic process assumes that the size of x_t ranges between two fixed bounds $L_1 < L_2$ for all time points t. The birth and death rates for the population are $\lambda_n = \alpha n(L_2 - n)$ and $\mu_n = \beta n(n - L_1)$. The sample paths of this process are similar to the one in Figure 9, where $N = 64, L_1 = 3N/4, L_2 = N, \alpha = 1, \beta = 1$. We observe that the values fluctuate between the two bounds.

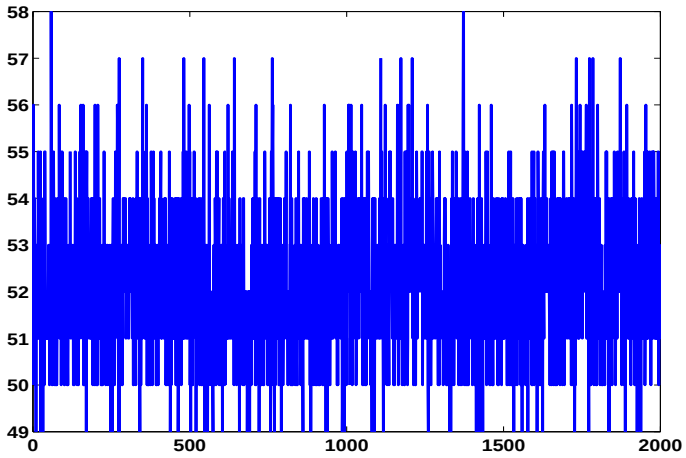

FIGURE 9. Sample path of x_t from a logistic process with the parameters $N = 64, L_1 = 3N/4, L_2 = N, \alpha = 1, \beta = 1$. We observe that the values fluctuate between the two bounds L_1 and L_2.

In the analysis we will restrict our attention to values of x_t that are not very large, since the model is valid mainly for low or moderate values of x_t.

First, the error analysis points out that if a sufficiently small number of nodes is to be updated at each time point, the error converges to zero very quickly. On the other hand, as the values of x_t increase, the error may or may not converge to zero, depending on the connectivity parameters. For example, if $N = 64$ we observe that if $x_t > N/2$ in the two-dimensional case, some combinations of the connectivity parameters generate errors that do not converge to zero. In order to have a better understanding of how the connectivity parameters affect the sensitivity to initial values, we employ three-dimensional graphs in which we plot the error $E(t)$ for $t = 5000$, against k_1 and k_2. In other words, we iterate the system 5000 times to surpass the transient states, and we only consider $E(5000)$. In Figure 10 the parameters are $N = 64, M_1 = N/2, L_1 = 3N/4, L_2 = N, \alpha = 1, \beta = 4$, and the values of k_1 and k_2 range between 1 and 63. The error is zero for many combinations of k_1 and k_2 but is nonzero for large

values of both k_1 and k_2. We also observe that even for certain smaller values of k_1 and k_2 the error is nonzero. Thus we may expect to see nontrivial bifurcation diagrams for values of the connectivity which yield a nonzero error.

If the number of nodes increases, the three-dimensional graphs are similar, but the range of connectivity values for which nonzero error plots occur becomes wider. At the same time, if all the connectivity parameters have very large values, the error converges to zero again. We can see this behavior in Figure 11 where $N = 256, M_1 = N/2, L_1 = 3N/4, L_2 = N, \alpha = 1, \beta = 4$, and the connectivity parameters range between 1 and 255. We see that for connectivity parameters between approximately 50 and 150 the error is nonzero, otherwise it is zero in most cases. The graph has a symmetric shape since $M_1 = N/2$.

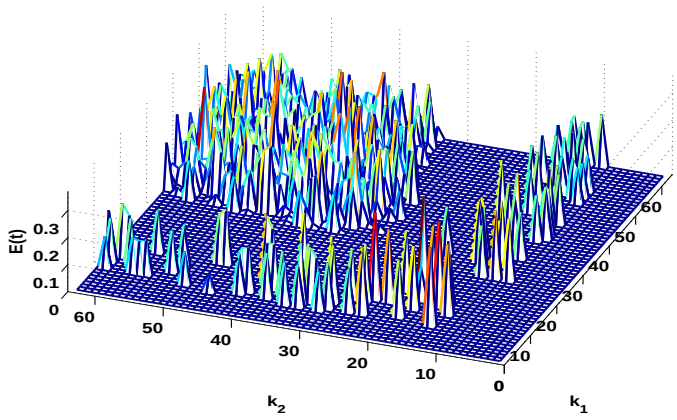

FIGURE 10. Error plot for the case of x_t from a logistic process with the parameters $N = 64, M_1 = N/2, L_1 = 3N/4, L_2 = N, \alpha = 1, \beta = 4$. We plot $E(5000)$ (meaning the error after 5000 iterations) against k_1 and k_2. The error is zero for many combinations of k_1 and k_2, but is nonzero for large values of both k_1 and k_2. We also observe that even for certain smaller values of k_1 and k_2 the error is still nonzero.

If M_1 decreases, the values of k_1 for which the system exhibits sensitivity to initial values decrease too. If M_1 increases, then the values increase too. So the three-dimensional error plots are not as symmetric as in Figures 10 and 11. They are very similar in all other aspects.

This situation is similar in the one-dimensional case. In Figures 12 and 13 we present three-dimensional graphs representing the plot of $E(t)$ against t and k. The parameters are $L_1 = 3N/4, L_2 = N, \alpha = 1, \beta = 4, N = 64$ and $N = 256$ respectively. The system is iterated 2^{11} time points. We observe that the error is nonzero for large values of k in both figures. However in Figure 12 some nonzero plots are observed also for values of k between 5 and 15

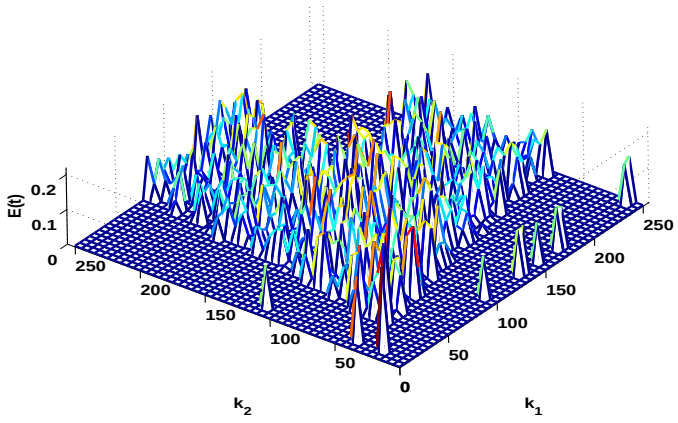

FIGURE 11. Error plot for the case of x_t from a logistic process with the parameters $N = 256, M_1 = N/2, L_1 = 3N/4, L_2 = N, \alpha = 1, \beta = 4$. We plot $E(5000)$ (meaning the error after 5000 iterations) against k_1 and k_2. For connectivity parameters between approximately 50 and 150 the error is nonzero, otherwise it is zero in most cases. The graph has a symmetric shape since $M_1 = N/2$.

with approximation, while in Figure 13 we observe that very large values of k lead to zero error in the long run. Thus the behavior is very similar to the two-dimensional case, suggesting that as the number of nodes increases, the range of values for which the error is nonzero becomes larger, and generally it contains larger values of the connectivity parameter. At the same time, if N becomes large enough, the error plots converge to zero for very large values of k as seen in Figure 13. In general, our simulations indicate that if the parameter combinations yield values of x_t that are at least $N/2$ with approximation, the error plots generate nonzero error for at least some connectivity values. As x_t increases, the range of k for which this phenomenon is observed becomes wider as indicated in the previously mentioned figures.

We turn now to the analysis of the bifurcation diagrams for values of the connectivity parameter(s) that correspond to the error plots presented earlier. The bifurcation diagrams indicate that for small or moderate values of x_t the system is ordered exhibiting stable fixed points of order one or two. For larger values of x_t and values of the connectivity parameters that indicate a nonzero error in the sensitivity analysis, the bifurcation diagrams indicate chaos through period-doubling bifurcations for larger connectivity values, as seen in Figure 14. The parameters are: $N = 64, M_1 = N/2, L_1 = 3N/4, L_2 = N, \alpha = 1, \beta = 4$ (as in Figure 10), while $k_1 = 4, 20$ and 50 respectively. According to the error plot, $k_1 = 4$ falls in the region where the error is zero, while the other ones do not. For this value the diagram shows one period-doubling bifurcation which

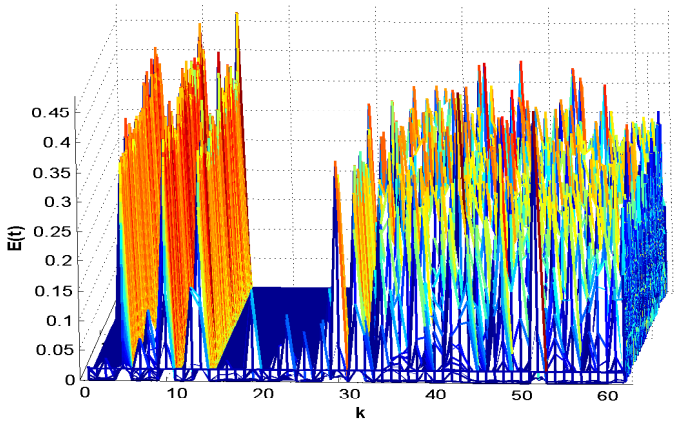

FIGURE 12. Error plot for the case of x_t from a logistic process with the parameters $N = 64, L_1 = 3N/4, L_2 = N, \alpha = 1, \beta = 4$. We plot 2048 iterations for each value of k. There is a wide range of values of k that generate the nonzero error plots. As the values of x_t increase this range becomes even wider.

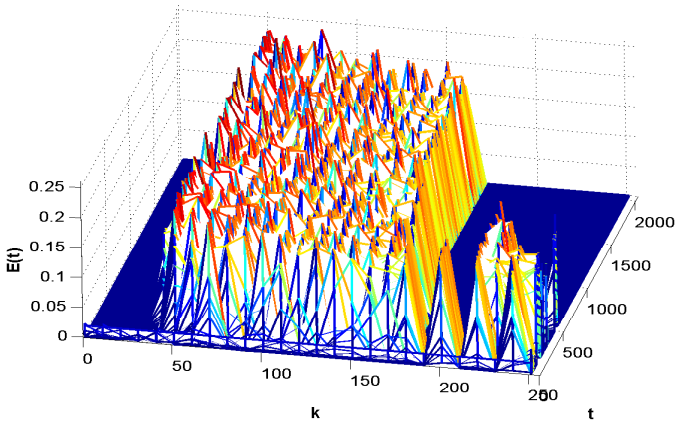

FIGURE 13. Error plot for the case of x_t from a logistic process with the parameters $N = 256, L_1 = 3N/4, L_2 = N, \alpha = 1, \beta = 4$. We plot 2048 iterations. There is a wide range of values of k that generate the nonzero error plots. However, if the connectivity values are very large, the error converges to zero again. As the values of x_t increase the range of k generating nonzero error becomes even wider. In general, error plots that do not converge to zero are observed for values of $x_t \geq N/2$ with approximation, regardless of the value of N.

is reversed. For $k_1 = 20$ the bifurcation is not reversed anymore, while for $k_1 = 50$ the system exhibits chaos if k_2 is large enough. We observe also the "gaps" in the bifurcation diagrams for values of k_2 between approximately 30 and 50 for $k_1 = 20$, and 20 and 30 for $k_1 = 50$. The

gaps suggest a single fixed point (besides zero). This figure allows us to understand how the bifurcation diagrams change as the connectivity parameter k_1 increases.

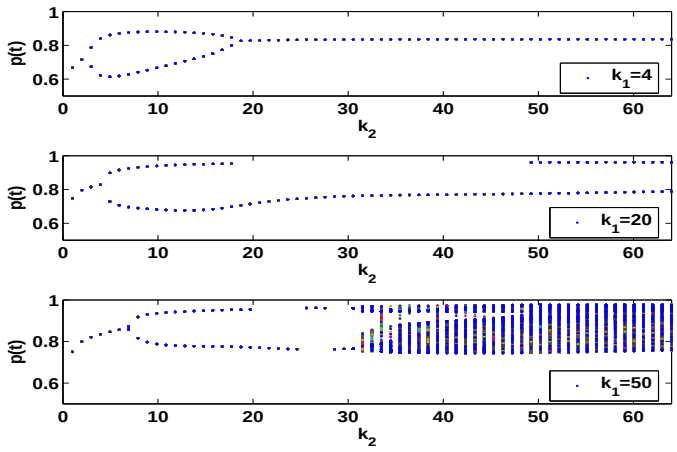

FIGURE 14. Bifurcation diagram for the case where x_t is from a logistic process. The parameters are set as follows: $N = 64, M_1 = N/2, L_1 = 3N/4, L_2 = N, \alpha = 1, \beta = 4$, and $k_1 = 4, 20$ and 50 respectively. According to the error plot, $k_1 = 4$ falls in the region where the error is zero, while the other two do not. For $k_1 = 4$ the diagram shows one period-doubling bifurcation which is reversed. For $k_1 = 20$ the bifurcation is not reversed anymore, while for $k_1 = 50$ the system exhibits chaos when k_2 is large enough. We observe also the "gaps" in the bifurcation diagrams for values of k_2 between approximately 30 and 50 for $k_1 = 20$, and 20 and 30 for $k_1 = 50$. The gaps suggest a stable fixed point.

In the one-dimensional case the situation is similar. For large enough values of x_t the system exhibits chaos if k is sufficiently large. Otherwise it exhibits stable fixed points or period-two stable orbits. As N increases, the chaos is reversed for large values of k, which corresponds to the zero error plots observed in Figure 13. We provide an example in Figure 15, where the three bifurcation diagrams correspond to $N = 64, 128$, and 256 respectively. The other parameters are the same in all three graphs, namely $L_1 = 3N/4, L_2 = N, \alpha = 1$, and $\beta = 4$. We iterate the system 3000 times before plotting the diagrams.

In conclusion, the values of x_t are again very important in the behavior of the system. If the values are small or medium, the system has an ordered behavior. If the values of x_t are larger, the system may exhibit chaos which may or may not be reversed depending on the other parameters of the system. In general, small connectivity generates order. Again, these results support the conclusions of (Matache, 2006) for the case of asynchrony generated by a fixed

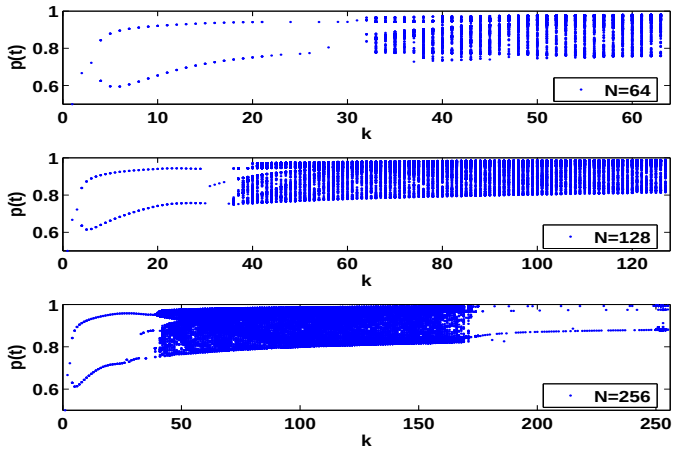

FIGURE 15. Bifurcation diagrams for the case where x_t is from a logistic process. The parameters are set as follows: $L_1 = 3N/4, L_2 = N, \alpha = 1, \beta = 4$, and $N = 64, 128$ and 256 respectively. We observe the ordered behavior for small values of k in all the graphs, and that the system exhibits chaos for large values of k which may be reversed if N is large. These diagrams correspond to the error plots presented earlier for the one-dimensional case.

distribution, rather than a stochastic process. If N is large enough then a very small or very large connectivity also generates order.

4.3. **Asynchrony Generated by a Poisson Process.** To analyze the dynamics of the system when the asynchrony is generated by a Poisson process, we start by considering the homogeneous process where the parameter λ is a constant. The first observation is that since at each time point t the value of x_t is a Poisson random variable with parameter λt, there is an increasing trend in the number of nodes to be updated as time goes by. In other words, the system will eventually reach synchrony and will not switch back to asynchrony. Thus, for practical purposes, we will consider mainly small values for λ to understand the asynchronous behavior of the system, and large values of λ to see what features we encounter for a synchronous system.

However, to make things more flexible, we will later expand the study to nonhomogeneous Poisson processes.

Now let us discuss the sensitivity of the orbits to initial values for a homogeneous Poisson process. Numerous simulations in the multidimensional case (with a varying number of parents) suggest that regardless of the values of x_t or the number of parents, the error usually converges to zero. The rate at which the error converges to zero may vary depending on the underlying parameters.

The situation is similar for the one-dimensional case (with a fixed number of parents for all nodes); the error is convergent to zero in most cases. This suggests that the system is in general not sensitive to changes in initial values and we may expect the bifurcation diagrams to exhibit stable fixed points.

Indeed, the bifurcation diagrams indicate that the system exhibits an ordered behavior for the multidimensional case. Figure 4 is typical for homogeneous Poisson processes as well.

In the one-dimensional case, we provide an example in Figure 16 where we graph a sample path for x_t with parameter $\lambda = 0.05$, together with two levels of the bifurcation diagrams. More precisely, we iterate the system $N/2$ times and N times respectively before plotting the bifurcation diagrams, to indicate more precisely the stages of the system before reaching a steady state. We also include a zoom-in on the diagram corresponding to $N/2$ iterations for more clarity. We observe that the system is ordered and converges to a stable fixed point in the long run. After $N/2$ iterations the system exhibits higher order fixed points.

Thus we can conclude that for the homogeneous Poisson process, the system is ordered regardless of the underlying parameters as long as it is mostly asynchronous.

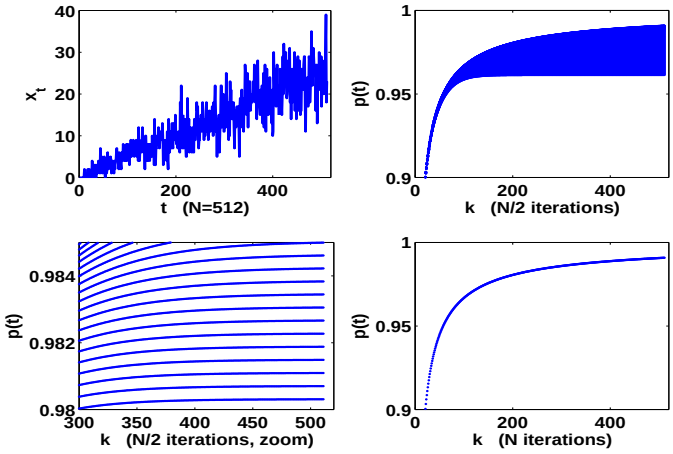

FIGURE 16. Bifurcation diagrams for the case of x_t from a Poisson process with $\lambda = 0.05$ and $N = 512$. The upper left graph is the sample path of x_t, the upper right is the bifurcation diagram graphed after $N/2$ iterations of the system, the lower left is a zoom in on the upper right graph, and the lower right is the bifurcation diagram after N iterations. We observe the ordered behavior, with higher order fixed points after $N/2$ iterations and one stable fixed point after N iterations. We include the case of $N/2$ iterations for a more complete view of the stages that the system passes before reaching a steady state.

If the intensity parameter is a power function of t, namely $\lambda(t) = \alpha t^{-\beta}$, with $\alpha \in [0, N]$ and $\beta > 1$ as specified earlier, the error converges to zero in all cases. If β is close to 1 the rate of convergence is slower and it could take a few thousand iterations before the error settles to zero. Therefore, in the bifurcation diagrams we iterate the system at least 3000 times before plotting the diagrams. We present an error plot together with a typical sample path in Figure 17. The parameters are as follows: $N = 512, M_1 = N/2, k_1 = 320, k_2 = 384, \alpha = N, \beta = 1.1$. This graph is typical. We observe the slow convergence to zero of the error plot. If β is larger, the error converges to zero very quickly.

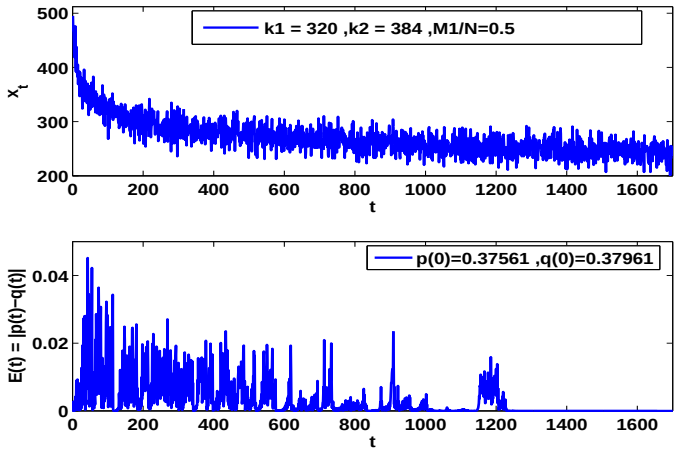

FIGURE 17. Error plot for the case of a nonhomogeneous Poisson process with a power function for the intensity parameter, namely $\lambda(t) = \alpha t^{-\beta}$, with $\alpha = N$ and $\beta = 1.1$. The upper graph is the sample path, and the lower graph represents the corresponding error plot. Here $N = 512, M_1 = N/2, k_1 = 320$ and $k_2 = 384$. We observe that for values of β close to 1, the error converges to zero slowly, as seen in this graph.

The bifurcation diagrams for this case are similar to Figure 4. These results hold in both the one-dimensional and the multidimensional cases.

In conclusion, when the asynchrony is generated by a Poisson process, the asynchronous system has an ordered behavior regardless of the values of x_t. This result emphasizes that other parameters can have an important impact on the behavior of the system. Thus, when stochastic processes are employed, the level of asynchrony may not be the one that influences the most the long-term behavior of the system.

4.4. **Asynchrony Generated by the Fractional Brownian Motion Process.** In this section we analyze the system dynamics with asynchrony generated by a FBM process with Hurst

parameter $1/2 \leq H < 1$. For $H = 1/2$ becomes the classical BM process. We include the BM process in this discussion as a special case of the FBM.

In the multidimensional case, the analysis of the sensitivity to initial values leads to the conclusion that in the case of the BM process, the error converges to zero in most cases. For large values of x_t and sufficiently small values of the connectivity parameters, the error may not settle, suggesting the possibility of chaos. The bifurcation diagrams support this conclusion. When the values of x_t are small or medium, then the graph of Figure 4 is valid also for the BM process. On the other hand, if the values of x_t are large, the system may exhibit chaos for smaller values of the connectivity parameters and order for larger values of the connectivity parameters, as seen in Figure 18 for $N = 512, M_1 = N/2$.

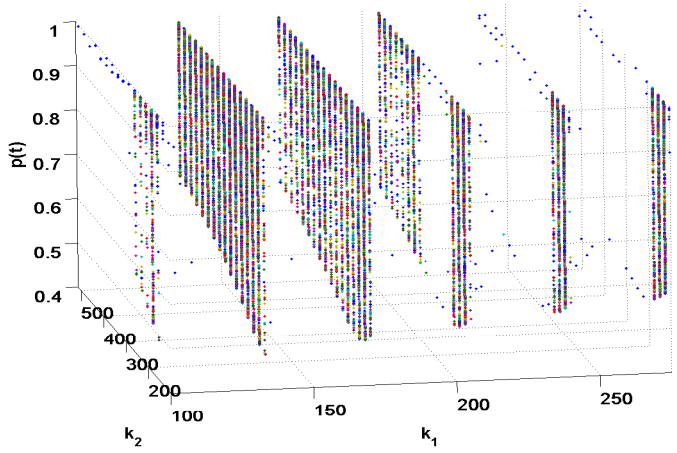

FIGURE 18. Bifurcation diagram for $N = 512, M_1 = \frac{N}{2}, M_2 = \frac{N}{2}$, and x_t from a BM process. The equations of the model are iterated 2000 times to eliminate any transient behavior. We plot the bifurcation diagrams of $p(t)$ versus k_2 for several values of k_1. The diagrams show that the system exhibits chaos for sufficiently small values of the connectivity parameters k_1 and k_2, and order for large connectivity parameters. In this figure we only show a few "slices" for various k_1 values that range between 100 and 300. For larger values the graphs are similar to the one for $k_1 = 300$ approximately, while for smaller values they exhibit stable fixed points.

In the one-dimensional case we observe again that the values of x_t are the most important factor in determining the dynamics of the system. The error converges to zero for small values of x_t and may or may not converge to zero for medium or large values of x_t depending on the connectivity parameter. The bifurcation diagrams clarify this. For small values of x_t the system exhibits stable fixed points, while for medium and large values of x_t it exhibits chaos through

period-doubling bifurcations and periodic windows. We include Figure 19 that corresponds to medium values of x_t as seen in the upper left graph representing the sample path of BM. We graph the bifurcation diagrams after $N/4, N$ and $10N$ iterations respectively. We can see that the diagrams exhibit chaos. On the other hand, in Figure 20, the system is mostly synchronous, and we can see that after $10N$ iterations the chaos occurs for only very small values of k, which is expected in a synchronous system as explained earlier in Section 4.1.

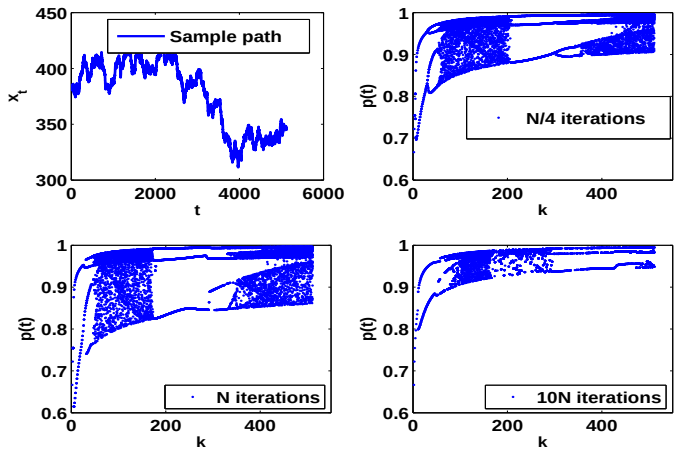

FIGURE 19. Bifurcation diagram for $N = 512$ and x_t from a BM process starting at $3N/4$. The sample path of x_t in the upper left graph shows that the values of x_t are medium. The diagrams show that the system exhibits chaos through period-doubling bifurcations and periodic windows. The system is iterated $N/4, N$ and $10N$ times respectively before plotting the diagrams to understand how the behavior changes with time.

Next we turn our attention to the FBM process with Hurst parameter $1/2 < H < 1$. Here we observe that the system exhibits sensitivity to initial values only for large values of x_t. Basically, as the Hurst parameter increases, the system exhibits ordered behavior for a wider range of x_t values. When H is close to $1/2$, the system exhibits chaos for larger values of x_t as seen in Figure 21, where $N = 512, M_1 = N/2$, and $H = 0.6$. Chaos is observed for all "slices" for different k_1 values, with periodic windows of various lengths, although in some cases chaos is observed only for small values of k_2. The diagrams may also exhibit reversed bifurcations. When H approaches 1 the system is mostly ordered. Chaos may occur for small values of the connectivity parameters and large values of x_t, and the graphs are similar to those for BM as in Figure 20.

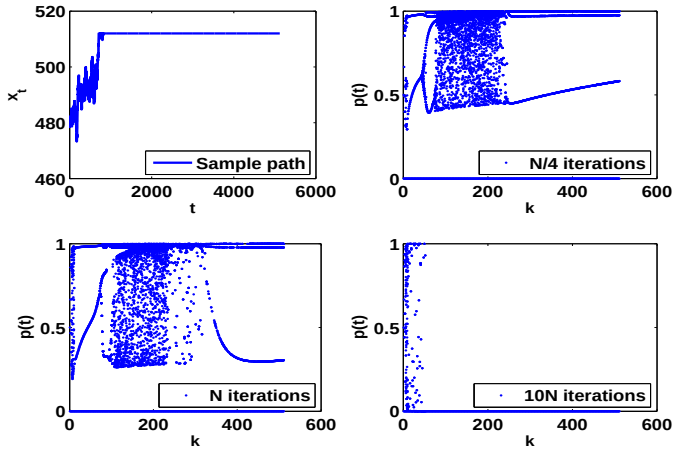

FIGURE 20. Bifurcation diagram for $N = 512$ and x_t from a BM process starting at $15N/16$. The sample path of x_t in the upper left graph shows that the values of x_t are very large, so the system is mostly synchronous. The bifurcation diagrams show that the system exhibits chaos through period-doubling bifurcations, which is reversed for higher values of k if the system is iterated $N/4$ or N times respectively before plotting the diagrams. However, in the long run, the chaos is observed only for very small connectivity, the system exhibiting order for most connectivity values.

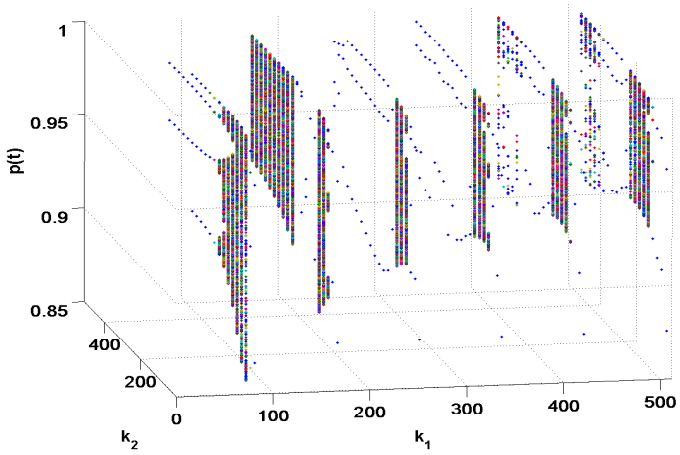

FIGURE 21. Bifurcation diagram for the case of $N = 512, M_1 = N/2$, and $H = 0.6$. Chaos is observed for all k_1 "slices" with periodic windows of various lengths, although in some cases chaos is observed only for small values of k_2. The diagrams may exhibit also reversed bifurcations.

In the one-dimensional case we observe again that as the Hurst parameter increases, the system exhibits order for a larger range of x_t values. For $H = 0.5$, which is the classical BM, the system exhibits chaos when the values of x_t are medium or large. When $H = 0.7$, for example,

the system exhibits chaos mainly for large values of x_t, while when $H = 0.9$ the system exhibits order for any values of x_t. Therefore the Hurst parameter is important in the dynamics of the system, as in the multidimensional case. For example, when $H = 0.7$ the system exhibits chaos for small values of k when x_t is large, and order otherwise. Figure 20 is valid again for large values of x_t, with possible differences in the width and length of the bifurcation diagram corresponding to chaos. For small or medium values of x_t the system exhibits stable fixed points. When $H = 0.9$ the system has only stable fixed points.

We have presented only the cases of the three H values as specified above ($H = 0.5, 0.7, 0.9$), but the system exhibits similar behavior for other values.

In conclusion, the values of x_t are again of importance in the BM case, generating mostly order and possibly chaos for very large values of x_t. In the FBM case, the Hurst parameter is also very important. If H is small (close to $1/2$), the system exhibits chaos for moderate or large values of x_t. As H increases the range of values of x_t that generate chaotic behavior reduces step by step. For very large values of H (close to 1), the system is ordered for any values of x_t (we exclude the synchronous case which was discussed in Section 4.1). These results show that although the values of x_t are important to a certain extent, the other parameters have also a great impact on the behavior of the system.

5. Conclusions

This paper provides a generalization and extension of the work proposed in (Matache and Heidel, 2005) and (Matache, 2006) where the authors study asynchronous random Boolean networks governed by the elementary cellular automata rule 126 under the assumption of asynchrony generated by given random variables. In this paper we extend those results by allowing a variety of stochastic processes as generators for the number of parents to be updated at each time point. Stochastic processes such as Poisson, random walk, birth and death and fractional Brownian motion are employed as the random number generator. The dynamics of the system show that the number of nodes to be updated at each time point is of great importance especially for the random walk, the birth and death, and the Brownian motion processes. Small or moderate values for the number of updated nodes generate order, while large values may generate chaos depending on the underlying parameters. This is agreement with previous results for the case when asynchrony is generated by a fixed random variable (Matache, 2006). The Poisson process generates order for any parameter combinations. In the case of the fractional

Brownian motion, the values of the Hurst parameter are very important. As the values of the Hurst parameter increase the system exhibits order for more combinations of the underlying parameters. In the synchronous case the results match the findings of (Andrecut and Ali, 2001) for the one-dimensional case, and (Matache and Heidel, 2004) for the multidimensional case. Thus, when dealing with stochastic processes, the level of asynchrony is important to a certain extent, but the other parameters may have a great impact on the behavior of the system.

It would be of interest to expand even further the analysis of dynamics of asynchronous random Boolean networks under other stochastic processes. For example, genetic models that allow for mutation of genes would be of interest in genetics and applications.

It has been observed that many processes in natural or artificial networks, could be both asynchronous and ordered or rhythmic (Cornforth et al., 2001), (Di Paolo, 2001). Asynchrony can happen at a local level, but the global system exhibits modularity. The authors of (Cornforth et al., 2001) propose the spotlight model in which the Boolean network is divided into modules, each module being associated to a regulator node which controls the updates of the module, depending on its own state. The amount of asynchrony is obtained by altering the number of modules used. Applying the spotlight model to the work described in this paper could generate some interesting results. On the other hand, considering the issue of analyzing the rhythmic or non-rhythmic attractors would be of interest and would extend recent studies (Di Paolo, 2001), (Rohlfshagen and Di Paolo, 2004).

Future work will focus on introducing "noise" in the system to study the stability of the system to perturbations. Robustness or sensitivity of networks to the variation of some internal parameters and to perturbations of the states of the system have been studied recently by various authors, e.g. (Aldana and Cluzel, 2003), (Bilke and Sjunnesson, 2001), (Shmulevich and Kauffman, 2004). In scale-free networks perturbing a very highly connected node is expected to have a much bigger impact than perturbing a node with low connectivity. Thus allowing also a power law distribution for the connectivity k could be of further interest for the study of the dynamical properties of scale-free networks in light of recent studies (Albert and Barabasi, 2000), (Aldana and Cluzel, 2003), (Barabasi et al., 1999).

Considering the issue of synchronization of networks is of interest based on works that point out the importance of the behavior of two or more elements with complex dynamics engaged into a synchronized state which generates a complex evolution itself (Morelli and Zanette, 1998), (Morelli and Zanette, 2001), (Zanette and Morelli, 2003). This feature has been observed in

biology, chemistry, neural networks, or social networks, where complex systems have been shown to evolve based on synchronization of coupled elements (Abarbanel et al., 1996), (Neda et al., 2000), (Winfree, 1980), (Zhigulin et al., 2003). Allowing the synchronization process to have random features, as well as considering variability in the initial states of the networks to be synchronized, are topics for future research.

Given the intrinsic connection between Boolean networks or cellular automata and neural networks (Aldana et al., 2003), (Anthony, to appear), (Kürten, 1988), a natural step would be to identify the dynamics generated using the approach of this paper in the case of a (linear or non-linear) Boolean threshold rule which is related to the functions computed by a linear or non-linear threshold neuron when its inputs are restricted to binary values. When the weighted sum of the inputs corresponding to a neuron is at least the threshold value, then the neuron fires, or is turned ON; otherwise it does not, or is OFF. Moreover, the usage of asynchrony in the evolution of the Boolean network allows one to understand the evolution of the so-called "Type A" spiking neurons with "binary encoding" in which the neurons have "active" and "non-active" periods (Anthony, to appear). At the same time in (Huepe and Aldana, 2002) the authors provide a study on the dynamical organization in the presence of noise of a Boolean neural network with random connections. A further direction would be to generate a similar study in the context of the network described in this paper, and to further extend the study to other Boolean threshold rules.

Another question related to neural networks is how to make evolvable (neural) networks that are reversible? The topic is of critical future importance for the field of brain building in particular and for computer science in general. A Boolean model is proposed in (De Garis et al., 2002). The authors impose several constraints on the Boolean rules: the number of parents equals the number of children for each node; there is a one-to-one correspondence between the input state and the output state of the network so that the steps can be reversed; the network is assumed synchronous. Studying the dynamics of a network under similar rule constraints but allowing a potential asynchrony could deepen the understanding of how to construct artificial brains by evolving neural networks with applications in areas such as electronics.

It would also be of interest to go one step further in this paper's generalization and allow for multiple Boolean rules to be used in the iterations of the system, thus surpassing the case of cellular automata. On the other hand, only changing the unique Boolean rule to be used based

on other cellular automata rules, especially the class of totalistic and legalistic rules (Wolfram, 2002), could lead to interesting new models and dynamic behaviors.

REFERENCES

Abarbanel H.D.I., Rabinovich M.I., Selverston A., Bazhenov M.V., *Synchronization in neural networks*, Phys.-Uspeki 39, 1996, p. 337-362

Albert R., Barabasi A-L., *Dynamics of complex systems: scaling laws for the period of Boolean networks*, Physical Review Letters, 84, 24 (2000), p. 5660-5663.

Aldana M., Cluzel P., *A natural class of robust networks*, PNAS 100 (15), 2003, p. 8710-8714.

Aldana M., Coppersmith S., Kadanoff L.P., *Boolean dynamics with random couplings*, Perspectives and Problems in Nonlinear Science. A celebratory volume in honor of Lawrence Sirovich, E. Kaplan, J. E. Marsden, and K. R. Sreenivasan, editors, Springer Applied Mathematical Sciences Series, Springer, 2003.

Andrecut M., Ali M. K., *Chaos in a simple Boolean network*, International Journal of Modern Physics B, Vol. 15, 1 (2001), p. 17-23.

Anthony M., *Probabilistic Learning of Boolean Functions*. To appear in Boolean Methods and Models (ed. Y. Crama and P.L. Hammer).

Barabasi A-L., Albert R., Jeong H., *Mean-field theory for scale-free random networks*, Physica A, 272 (1999), p. 173-187.

Beran J., *Statistics for long-memory processes*, Chapman-Hall, New York, 1994.

Bilke S., Sjunnesson F., *Stability of the Kauffman model*, Phys. Rev. E 65 (1), 2001, 016129.

Boccara N., Roblin O., Roger M., *Route to chaos for a global variable of a two-dimensional 'game-of-life' automata network*, Journal of Physics A: Math. Gen, 27 (1994), p. 8039-8047.

Cornforth, D., Green, D.G., Newth, D., Kirley, M.R., *Ordered asynchronous processes in natural and artificial systems*, P. Whigham et al. (eds). Proceedings of the 5th Australia-Japan Joint Workshop on Intelligent & Evolutionary Systems, The University of Otago, Dunedin, New Zealand, 2001, p. 105-112.

Cornforth D., Green D.G., Newth D., Kirley M., *Do artificial ants march in step? Ordered asynchronous processes and modularity in biological systems* , Artificial Life VIII, MIT Press, 2002, p. 28-32.

De Garis H., Dinerstein J., Sriram R., *A Reversible Evolvable Network Architecture and Methodology to Overcome the Heat Generation Problem in Molecular Scale Brain Building*, GECCO Late Breaking Papers, Erick Cant-Paz (Ed.), AAAI 2002, p. 83-90.

Di Paolo E.A., *Rhythmic and non-rhythmic attractors in asynchronous random Boolean networks*, BioSystems, 59, 2001, p. 185-195.

Duncan T.E., Hu Y., Pasik-Duncan B., *Stochastic calculus for fractional Brownian motion*, SIAM Journal on Control and Optimization, 38, 2 (2000), p. 582-612.

Flyvbjerg H., Kjaer N.J., *Exact solution of Kauffman's model with connectivity one*, Journal of Physics A: Math. Gen., 21 (1988), p. 1695-1718.

Fogelman-Soulie F., Goles-Chacc E., Weisbuch G., *Specific roles of the different Boolean mappings in random networks*, Bulletin of Mathematical Biology, Vol. 44, 5 (1982), p. 715-730.

Fogelman-Soulie F., *Frustration and stability in random Boolean networks*, Discrete Applied Mathematics, 9 (1984), p. 139-156

Fox J.J., Hill C.C., *From topology to dynamics in biochemical networks*, Chaos, Vol. 11, 4 (2001), p. 809-815.

Gershenson C., *Classification of Random Boolean Networks*, Artificial Life VIII, Standish, Abbass, Bedau (eds) (MIT Press), 2002, p. 1-8.

Harvey I., Bossomaier T., *Time out of joint: attractors in asynchronous random Boolean networks*, Proceedings of the Fourth European Conference on Artificial Life (ECAL97), MIT Press, 1997, p. 65-75.

Heidel J., Maloney J., Farrow C., Rogers J.A., *Finding cycles in synchronous Boolean networks with applications to biochemical systems*, International Journal of Bifurcation and Chaos, 13 (2003), p. 535-552.

Huang S., *Genomics, complexity and drug discovery: insights from Boolean network models of cellular regulation*, Pharmacogenomics, 2, 3 (2001), p. 203-222.

Huepe C., and Aldana-González M., *Dynamical Phase Transition in a Neural Network Model with Noise: An Exact Solution*, Journal of Statistical Physics 108 (3/4), 2002, p. 527-540.

Kanada Y., *The effects of randomness in asynchronous 1D cellular automata*, Proceedings of ALIFE IV, 1994.

Kauffman S.A., *The origins of order*, Oxford University Press, 1993, p. 173-235.

Kürten K.E., *Correspondence between neural threshold networks and Kauffman Boolean cellular automata*, J. Phys. A: Math. Gen (21), 1988, L615-L619.

Leland W.E., Taqqu W.S., Willinger W., Wilson D.V., *On the self-similar nature of Ethernet Traffic*, IEEE/ACM Transactions on Networking, 2, 1 (1994), p. 1-15.

Low S., Lapsley D., *Optimization flow control, i: Basic algorithm and convergence*, IEEE/ACM Transactions on Networking, 1999.

Matache M.T., Heidel J., *A random Boolean network model exhibiting deterministic chaos*, Phys. Rev. E 69, 056214, 2004, 10 pages.

Matache M.T., Heidel J., *Asynchronous random Boolean network model based on elementary cellular automata rule 126*, Phys. Rev. E 71, 026232 (2005), 13 pages.

Matache M.T., Matache V., *Queuing Systems with Multiple FBM-Based Traffic Models*, ANZIAM J., 46 (2005), p. 361-377.

Matache M.T., *Asynchronous Random Boolean Network Model with Variable Number of Parents based on Elementary Cellular Automata Rule 126*, IJMPB, Vol. 20, 8 (30 March 2006), p. 897-923.

Morelli L.G., Zanette D.H., *Synchronization of stochastically coupled cellular automata*, Phys. Rev. E 58 (1), 1998, R8.

Morelli L.G., Zanette D.H., *Synchronization of Kauffman networks*, Phys. Rev. E 63, 2001, 036204-1.

Neda Z., Ravasz E., Vicsek T., Brechet Y., Barabasi A.L., *Physics of the rhythmic applause*, Phys. Rev. E 61, 2000, p. 6987-6992.

Rohlfsagen P., Di Paolo E.A., *The circular topology of rhythm in asynchronous random Boolean networks*, BioSystems, 73(2), 2004, p. 141-152.

Ross S.M., *Stochastic processes*, John Wiley & Sons, 1983, p. 31-54.

Schönfisch B., De Roos A., *Synchronous and asynchronous updating in cellular automata*, BioSystems, 51(3), 1999, p. 123-143.

Sherlock R.A., *Analysis of the behaviour of Kauffman binary networks - I. State space description and the distribution of limit cycle lengths*, Bulletin of Mathematical Biology, Vol. 41 (1979), p. 687-705.

Shmulevich I., Dougherty E.R., Kim S., Zhang W., *Probabilistic Boolean networks: a rule-based uncertainty model for gene regulatory networks*, Bioinformatics, Vol. 18, 2 (2002), p. 261-274.

Shmulevich I., Kauffman S.A., *Activities and sensitivities in Boolean network models*, Physical Review Letters 93 (4), 2004, 048701.

Silvescu A., Honavar V., *Temporal Boolean network models of genetic networks and their inference from gene expression time series*, Complex Systems, 13 (2001), p. 61-78.

Stark W.R., Hughes W.H., *Asynchronous, irregular automata nets: the path not taken*, BioSystems, 55, 2000, p. 107-117.

Stauffer D., *Percolation thresholds in square-lattice Kauffman model*, Journal of Theoretical Biology, 135 (1988), p. 255-261.

Taylor H.M., Karlin S., *An introduction to stochastic modeling*, Academic Press, 1998, p. 267-331.

Thomas R., ed., *Kinetic Logic: A Boolean approach to the analysis of complex regulatory systems*, Lecture Notes in Biomathematics, Springer Verlag, 29 (1979).

Willinger W., Paxson V., Taqqu M.S., *Self-similarity and heavy tails: structural modeling of network traffic*, A practical guide to heavy tails: statistical techniques and applications, R. Adler, R. Feldman and M.S. Taqqu, editors, Boston, 1998.

Winfree A.T., *The geometry of biological time*, Springer, Berlin, 1980.

Wolfram S., *A new kind of science*, Wolfram Media, Champaign, 2002, p. 51-114.

Yin Z.-M., *New methods for simulation of fractional Brownian motion*, Journal of Computational Physics, 127 (1996), article 0158, p. 66-72.

Zanette D.H., Morelli L.G., *Synchronization of coupled extended dynamical systems: a short review*, International Journal of Bifurcation and Chaos 13 (4), 2003, p. 1-16.

Zhigulin V.P., Rabinovich M.I., Huerta R., Abarbanel H.D.I., *Robustness and enhancement of neural synchronization by activity-dependent coupling*, Physical Review E 67(2-1), 021901 (2003).